



Passive Control with Blade-End Slots and Whole-Span Slot in a Large Camber Compressor Cascade

H. Wang, B. Liu[†] and B. Zhang

School of Power and Energy, Northwestern Polytechnical University, Xi'an, Shaanxi, 710072, P. R. China

[†]*Corresponding Author Email: liubo704@nwpu.edu.cn*

(Received August 12, 2020; accepted September 24, 2020)

ABSTRACT

Suitable slot structure of the compressor blade can generate high-momentum jet flow through pressure difference between the pressure and suction surface, it has been proved that the slot jet flow can reenergize the local low-momentum fluid to effectively suppress the flow separation on the suction surface. In order to explore a slotted method for better comprehensive suppressing effects on the boundary layer separation near blade midspan and the three-dimensional corner separation, a diffusion stator cascade with large camber angle is selected as the research object. Firstly, the Slotted_1 and Slotted_2 whole-span slotted schemes are set up, then the Slotted_3 scheme with whole-span slot and blade-end slots is proposed, finally the performance of original cascade and slotted cascades is computed under a wide range of incidence angles at the Mach number of 0.7. The results show that: in the full range of incidence angles, compared with the whole-span slotted cascades, the development of the endwall secondary flow on the suction surface of Slotted_3 cascade is effectively suppressed, the degree of the mutual interference between the secondary flow and the main flow is reduced. Besides, on the suction surface of Slotted_3 cascade, the boundary layer separation near blade midspan and the corner separation are basically eliminated. As a result, compared with those of original cascade, the total pressure losses of Slotted_3 cascade are reduced in the full range of incidence angles, and its operating range of incidence angles is broadened. Moreover, compared with the whole-span slotted schemes, Slotted_3 scheme has a better adaptability to wide range of incidence angles.

Keywords: High-momentum jet; Boundary layer separation; Three-dimensional corner separation; Whole-span slot; Blade-end slots; Total pressure loss.

NOMENCLATURE

AO	axial overlap	y	pitchwise direction
C	chord length	β_{1k}	inlet angle
Ca	axial chord length	β_{2k}	outlet angle
H	blade height	β_S	stagger angle
L1	axial outlet position of slot	$\bar{\omega}$	total pressure loss coefficient
LE	Leading Edge	σ	total pressure recovery coefficient
N	node point		
P_{01}	inlet total pressure	Subscript	
P_{02}	local total pressure	hv	horseshoe vortex
P_1	inlet static pressure	LS	separation line
R	lower surface radius of slot	t	trailing edge
S	saddle point	e	endwall
t	blade pitch	cvs	suction side of corner vortex
TE	Trailing Edge	cr	critical value
x	spanwise direction	min	minimum
X	throat width of slot		

1. INTRODUCTION

As one of the core components of aeroengine, the compressor has been developing in the direction of high efficiency, high load and large mass flow in recent years (Eshraghi *et al.* 2016). At present, there are some design methods that can increase the load of compressor blades, one of which is the design of large camber angle. It can increase the load and the pressure diffusion capacity of the blade, thereby reducing the number of stages in compressors. However, the increase of load will intensify the flow separation inside compressors, resulting in an increase of total pressure loss, a reduction of efficiency and the narrowing of the safe operating range of compressors. Therefore, it is necessary to use reasonable flow control methods (Lord 2000) to suppress the flow separation on the surface of compressor blades and improve the aerodynamic performance of compressors (Beselt *et al.* 2014; Lei *et al.* 2008; Zhang *et al.* 2014).

The internal flow control methods of compressors are mainly divided into: (1) Active control methods, which include boundary layer suction (Mao *et al.* 2018; Zhang *et al.* 2020), plasma excitation (Akcaoz *et al.* 2016), etc. (2) Passive control methods, which include end-bend blade (Kan *et al.* 2020), casing treatment (Cevik *et al.* 2016), vortex generator (Hergt *et al.* 2012; Ma *et al.* 2018) and slotted blade, etc. However, compared with the active control methods, the passive control methods don't need extra complicated additional devices. By contrast, the passive control methods are simple and easy to implement and have certain cost-effectiveness, so the passive control methods remain preferable.

For slotted blade, its suitable slot structure can generate high-momentum jet flow through pressure difference between the blade pressure and suction surface, the jet flow can effectively suppress the flow separation on the suction surface. Therefore, many scholars have done a lot of researches on slotted blade. Rockenbach *et al.* (1968; 1970) applied slot structure on the blades of a compressor and conducted experimental studies to verify the applicability of the slotted blades in the compressor. Zhou *et al.* (2008; 2009; 2010) designed a two-stage turning slot structure and investigated the influence of slot outlet position and jet flow angle on the performance of the slotted cascade. Besides, the slot structure was applied to the stator blades of a single-stage compressor. It was found that due to the application of the slotted stator blades, the pressure ratio and efficiency of the single-stage compressor were increased.

Moreover, Ramzi *et al.* (2013) studied the slotted cascade under stall condition and analyzed the influence of the position, width and slope of the slot on its performance. Liu *et al.* (2016) applied slot structure to blade end and studied the influence of consistency and aspect ratio on the performance of the blade-end slotted cascade. The results showed that the blade-end slots could effectively suppress the three-dimensional corner separation and reduce the

total pressure loss, and the operating range of incidence angles was broadened. Tang *et al.* (2019) adopted two blade-end slots with different axial positions on a highly loaded compressor cascade, which achieved effective suppress on a large scope of three-dimensional corner separation. In the study, the loss coefficient could be reduced by 39.4% under the incidence angle of 4° , the results proved that the slot structure could effectively suppress the flow separation on the suction surface of the blade.

Studies have shown that when the outlet position of slot is located before and relatively close to the separation point on the suction surface of the blade, the suppressing effect on flow separation is better (Zhou *et al.* 2008). However, for the original blade with a large degree of flow separation on the suction surface, there is often a certain distance between the starting point of the corner separation line and the midspan boundary layer separation line. Under this circumstance, the whole-span slot has a limited comprehensive suppressing effect on the boundary layer separation near blade midspan and the three-dimensional corner separation.

In order to explore a slotted method for better comprehensive suppressing effects on the boundary layer separation near blade midspan and the three-dimensional corner separation, the slotted scheme with whole-span slot and blade-end slots is proposed, as a comparison, two whole-span slotted schemes are set up. Afterwards, the performance of original cascade and slotted cascades is computed in a wide range of incidence angles at a constant Mach number. At last, the effects of different slotted schemes on the total pressure loss, wake loss and flow turning angle are analyzed and compared, which reflect the aerodynamic performance of the compressor cascade.

2. CASCADE MODELS AND NUMERICAL METHODS

2.1 Original Cascade Model

In this study, a diffusion stator cascade with a large camber angle of 53.38° has been selected for the investigation of the flow separation control. The blade profile of the cascade is a multi-arc blade profile, and the camber of the middle arc is more concentrated on the second half of the blade. When the inlet Mach number of incoming flow is 0.7, the boundary layer separation near blade midspan on the suction surface and the three-dimensional corner separation are serious. Detailed geometric and aerodynamic parameters of the cascade are shown in Table 1.

2.2 Slotted Cascade Models

The geometry of the slot configuration used in this study is shown in Fig. 1. Line AB and line CD represent the upper and lower boundary of the slot, respectively, and L1 represents the outlet position of the slot. Moreover, the slot length is 40% of axial chord length (Ca), and the inlet and outlet widths of the slot are $0.25Ca$ and $0.15Ca$, respectively. In order to introduce the main flow of the blade pressure side

into the slot without additional losses, line AB is set to tangent to the pressure surface at point A (Liu *et al.* 2016). According to Denton's analysis (1993), the mixing losses caused by the slot jet and the main flow are closely related to the jet angle. The larger the slot jet angle, the greater the corresponding mixing losses. Hence, in order to effectively suppress the flow separation and reduce the mixing losses, compared with the direction of the main flow, the slot jet angle should be limited as small as possible (it is better to be consistent with the main flow direction). Therefore, line AB and line CD are set to tangent to the suction surface at point B and point D, respectively, and the axial overlap AO is as large as $0.15Ca$ to ensure that the slot jet flow direction is as consistent as possible with the main flow direction (Tang *et al.* 2019). For the aim to ensure the Coanda effect (Jones *et al.* 2002), the ratio X/R between the slot throat width X and the slot lower wall outlet curve radius R is kept at a small value of 0.04, ensuring that the high-momentum jet from the slot remains attached to the curved surface.

Table 1 Design parameters of the cascade

parameters	values
Chord C/mm	63
Blade height H/mm	100
Aspect ratio H/C	1.59
Blade pitch t/mm	43.15
Blade solidity C/t	1.46
Stagger angle $\beta_s/(^\circ)$	15.4
Inlet angle $\beta_{1k}/(^\circ)$	40.17
Outlet angle $\beta_{2k}/(^\circ)$	-13.21

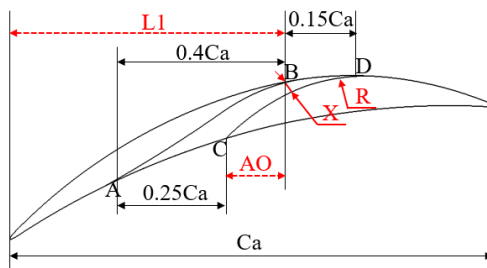


Fig. 1. Geometry of slot configuration.

Three slotted schemes are set up in this study, whose names are Slotted_1, Slotted_2 and Slotted_3 schemes, respectively. Slotted_1 and Slotted_2 schemes are whole-span slotted schemes, and Slotted_3 scheme is the slotted scheme with a whole-span slot and two blade-end slots. The study of Zhou *et al.* (2008) showed that when the outlet position of slot is located before and relatively close to the separation point on the suction surface, the suppressing effect on flow separation is better. For the original cascade, when the inlet Mach number and incidence angle are 0.7 and 0° , respectively, the axial position of the midspan separation line on the suction surface is about $0.87Ca$, and the axial position of the starting point of the corner separation

line is $0.3Ca$. Moreover, as incidence angle increases, the separation line moves toward the leading edge of the blade.

Based on above analyses, in order to achieve a better suppressing effect on the corner separation, the slot outlet of Slotted_1 cascade is set relatively close to the starting point of the corner separation line, that is, $L1$ is taken as $0.6Ca$. For the same purpose, the $L1$ of Slotted_2 cascade is taken as $0.8Ca$, that is, the slot outlet is set before the midspan boundary layer separation line to effectively suppress the boundary layer separation near blade midspan. The three-dimensional geometric model of Slotted_3 cascade is shown in Fig. 2, it can be seen that for the aim to better suppress the development of the endwall secondary flow on the suction surface, two blade-end slots are set up before the whole-span slot, and the height and axial outlet position of the blade-end slots are respectively 10% of blade height (H) and $0.55Ca$.

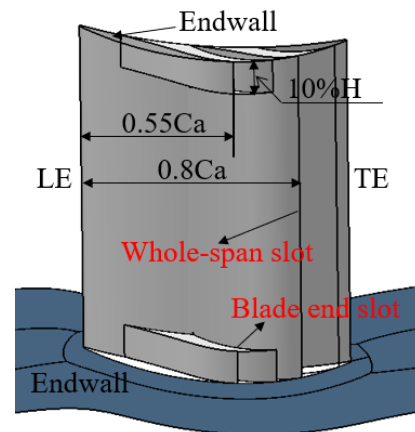


Fig. 2. Three-dimensional geometric model of Slotted_3 cascade.

2.3 Grid and Numerical Technique

In this study, a structured O4H mesh topology is automatically generated by the Autogrid5 module of the NUMECA software for the cascade passage, which contains 1.5 million grid points. And for the slot, a structured H mesh topology is manually generated by the IGG module of the NUMECA software. To ensure the reliability of the comparison of computational results, the number of grid points in the slot structure remains consistent, which is 0.38 million. Afterwards, a complete non-matching connection is adopted between the slot grid and the cascade passage grid. It ensures the validity of the numerical value transfer during computation. Additionally, both of the blade and the endwall are set to be non-slip adiabatic walls. Figure 3 shows the representative computational grid of Slotted_2 cascade with a whole-span slot. The inlet and outlet planes are respectively located at $1.0C$ upstream of the blade leading edge and $1.5C$ downstream of the blade trailing edge. The mesh can be duplicated along the spanwise direction into 181 planes (whole span) to obtain 3D mesh

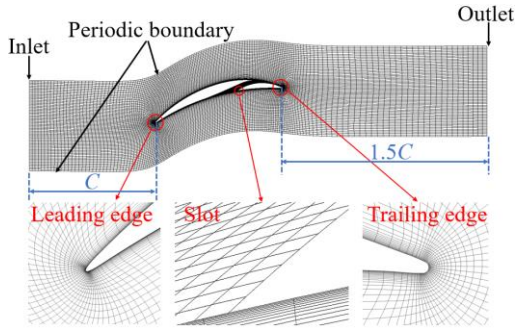


Fig. 3. Computational grid for Slotted_2 cascade.

In this study, the inlet Mach number is selected as a constant value of 0.7. In order to compare the performance of original cascade and slotted cascades in the operating range of incidence angles, the inlet incidence angle range is selected as -8° to 6.5° . Besides, the inlet total temperature and total pressure are respectively selected as 288.15K and 101325Pa. Since the slot jet direction is basically consistent with that of the main flow, its influence is limited to the single blade passage, one blade passage is simulated and the periodic boundary condition is set on both sides of the flow passage in this study. Afterwards, the Euranus solver is used to numerically solve the computational examples, and the steady-state computational method is adopted to solve the Navier-Stokes equation in the absolute coordinate

The Spalart-Allmaras turbulence model is adopted in the numerical computational process, in order to verify the validity of the Spalart-Allmaras turbulence model and the numerical method adopted in this paper, the performance of original cascade (Blade solidity $C/t=1.66$) is computed under 0.5° incidence angle at the Mach number of 0.6, and the comparisons between the computational results and the experimental results are performed. Figure 5 shows the computational results and the experimental results. It can be found that the numerical computational results are basically consistent with the experimental data, which proves that the numerical method adopted in this paper is reliable.

3. RESULTS AND DISCUSSION

3.1 Performance Analysis under 0° Incidence Angle

Since the flow structure of linear stator cascade is symmetrical about the 50%H plane of the blade, in order to highlight the details of the flow field, the performance of the cascades is analyzed within 0-50%H in this study. Figure 6 shows the flow structures on the suction surface and endwall of original cascade and three slotted cascades under 0° incidence angle. In the diagrams of limiting streamlines, the zone of red streamlines on the suction surface represent the influencing zone of the endwall secondary flow, and the blue streamlines represent the main flow. Figure 6(a) shows the limiting streamlines on the suction surface and endwall of original cascade and their topological

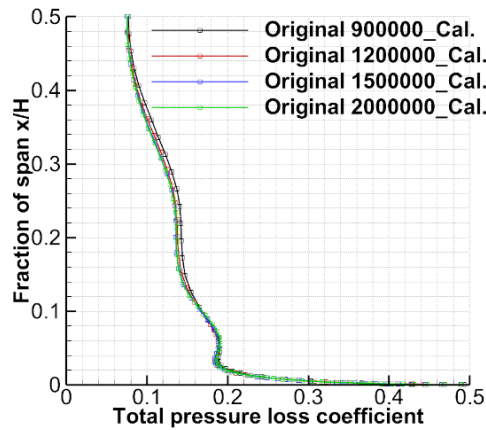
system. In the computational process, the central difference format with second-order accuracy is adopted as the spatial discretization format, the multi-grid acceleration technology and implicit residual smoothing method are used to accelerate the computational convergence.

Due to the wide incidence angle range of the computational conditions, the grid independences of original cascade and slotted cascades are verified under the condition with large degree of separation. The definition of total pressure loss coefficient is shown in Eq. (1), where P_{01} and P_1 respectively represent the inlet total pressure and static pressure, and P_{02} is the local total pressure. Figure 4(a) shows the spanwise distribution of pitchwise averaged total pressure loss coefficients of original cascade at outlet under 6° incidence angle. It can be seen that when the grid points exceed 1.2 million, the computational results of original cascade tend to be converged. For Slotted_2 cascade, the number of the cascade passage grid points is kept unchanged as 1.5 million, Fig. 4(b) shows the spanwise distribution of pitchwise averaged total pressure loss coefficients of the outlet plane under three different slot grid numbers, it can be found that the computational results show little difference when the slot grid number reaches 0.2 million.

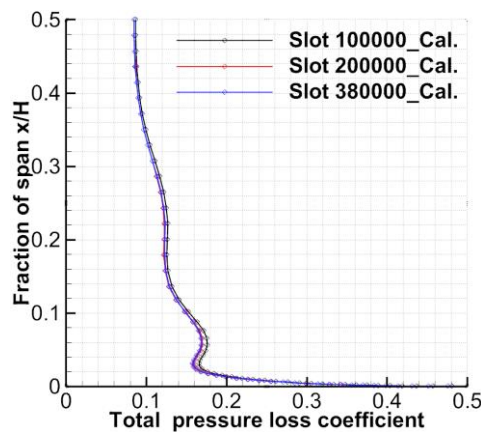
$$\bar{w} = \frac{P_{01} - P_{02}}{P_{01} - P_1} \quad (1)$$

structure. The analytic method for topological structure used in this study has been successfully used by Kan *et al.* (2019). It can be found from Fig. 6(a) that the suction side leg of horseshoe vortex firstly starts from saddle point S_{HV} and develops toward the suction surface direction under the action of crosswise pressure gradient, then it develops toward the midspan direction on the suction surface from the axial position of $0.3Ca$ and finally ends at node N_{LS} . Therefore, the scope of the corner separation is large, and the endwall secondary flow basically develops to 34%H on the suction surface of the blade. In addition, the main flow also separates on the suction surface before the blade trailing edge because of the action of reverse pressure gradient. All in all, the separation degree on the suction surface of original cascade is serious.

Figure 6(b) shows the limiting streamlines on the suction surface and endwall of the three slotted cascades. For Slotted_1 cascade, its slot outlet is set relatively close to the starting point of the corner separation line, which has a great suppressing effect on the development of the endwall secondary flow on the suction surface. As shown in the limiting streamline diagram of slotted_1 cascade, the development of the secondary flow from endwall to blade midspan on the suction surface is inhibited. However, since the slot outlet is far from the trailing edge of the blade and the camber of the middle arc is more concentrated on the second half of the blade, the main flow passing through the slot outlet separates in front of the trailing edge on the suction surface. Besides, the flow in the corner area also separates before the trailing edge to form shedding vortices.



(a) Original cascade



(b) Slotted_2 cascade

Fig. 4. Spanwise distribution of total pressure loss coefficients for different grid numbers under 6° incidence angle.

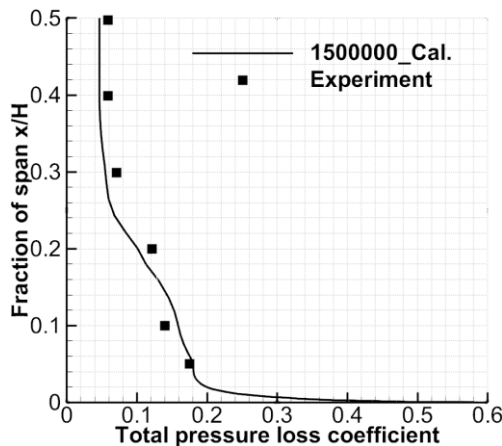


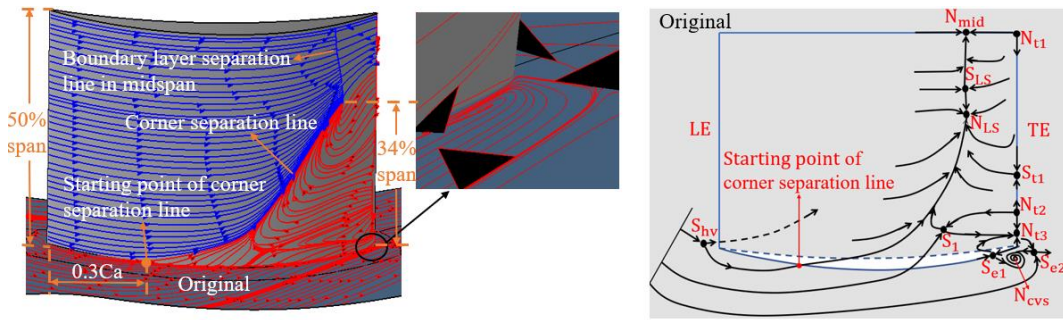
Fig. 5. Spanwise distribution of total pressure loss coefficients for original cascade under 0.5° incidence angle at the Mach number of 0.6.

The slot outlet of Slotted_2 cascade is located before the boundary layer separation line near blade midspan, it is relatively close to the trailing edge. Compared with Slotted_1 cascade, the boundary layer separation near blade midspan on the suction surface of Slotted_2 cascade is basically eliminated. But the development scope of the endwall secondary

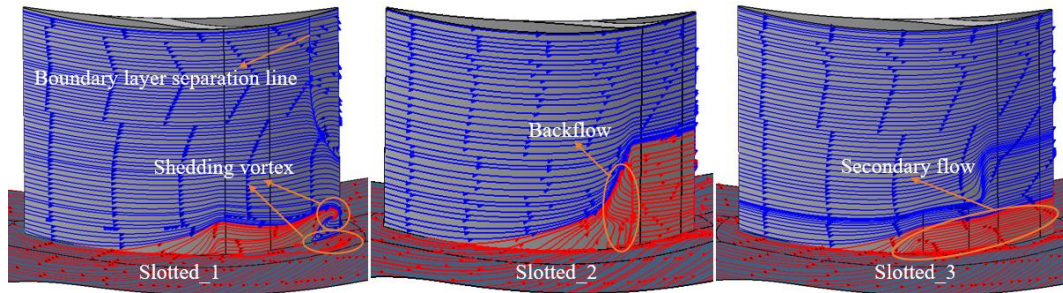
flow on the suction surface is enlarged, and a certain scope of backflow is formed in front of the slot outlet on the suction surface. However, due to the action of the slot jet, the separated flow is attached to the suction surface again after flowing through the slot outlet and flows along the suction surface to the trailing edge without separation. Compared with Slotted_2 cascade, the development of the endwall secondary flow on the suction surface of Slotted_3 cascade is suppressed better, due to the effect of its blade-end slot jet. The development scope of the secondary flow on the suction surface is reduced by the blade-end slot jet, which weakens the mutual interference between the secondary flow and the main flow. Compared with Slotted_1 cascade, the whole-span slot jet of Slotted_3 cascade suppresses the separation of the main flow on the suction surface. Besides, the whole-span slot jet reenergizes the secondary flow passing through the blade-end slot outlet, so that the secondary flow flows along the suction surface to the trailing edge without separation. Under 0° incidence angle, it can be concluded that compared with the whole-span slotted schemes, Slotted_3 scheme has a better comprehensive suppressing effect on the boundary layer separation near blade midspan and the three-dimensional corner separation.

Figure 7 shows the spanwise distribution of pitchwise averaged flow turning angles of the outlet plane under 0° incidence angle for the four cascades. Combined with the analysis of Fig. 6, it can be found that since the three slotted schemes have certain suppressing effects on the corner separation, the flow turning angles of them in the range of 0-30% H are increased compared with those of original cascade. However, for Slotted_1 cascade, because of the boundary layer separation near blade midspan before the trailing edge and the mixing effect of the slot jet and the main flow, its flow turning angles are decreased in the 30%-50% H interval. For Slotted_2 and Slotted_3 cascades, the flow turning angles of both are increased within the whole span compared with those of original cascade. Besides, compared with Slotted_2 cascade, the development of the secondary flow on the suction surface of Slotted_3 cascade is effectively inhibited, which weakens the mutual interference between the secondary flow and the main flow. Therefore, the flow turning angles of Slotted_3 cascade have a further increase within the whole span. In summary, compared with those of the whole-span slotted cascades, the flow turning angles of Slotted_3 cascade are increased further within the whole span, and the pressure diffusion capacity of Slotted_3 cascade is improved further.

The passage total pressure loss contours of the four cascades under 0° incidence angle are shown in Fig. 8. It can be seen that on S1-S5 planes, the total pressure losses of the three slotted cascades are reduced compared with those of original cascade. The slot jet of Slotted_1 cascade has a better suppressing effect on the flow separation near the slot outlet, which makes the total pressure losses on S2 and S3 planes smaller than those of Slotted_2 and Slotted_3 cascades. But the losses of slotted_1 cascade are higher on S4 and S5 planes, due to the



(a) Flow structures of suction surface and endwall for original cascade



(b) Flow structures of suction surface and endwall for three slotted cascades

Fig. 6. Flow structures of suction surface and endwall for original cascade and slotted cascades under 0° incidence angle.

mixing losses of the slot jet and the main flow and the losses caused by flow separation. Consistent with the analysis of Fig. 6, the blade-end slot jet of Slotted_3 cascade suppresses the development of the endwall secondary flow on the suction surface better, which reduces the development scope of the secondary flow on the suction surface and weakens the mutual interference between the secondary flow and the main flow. Slotted_3 scheme has a better comprehensive suppressing effect on the boundary layer separation near blade midspan and the corner separation, compared with Slotted_2 scheme. Therefore, the losses of Slotted_3 cascade on S2-S5 planes are lower than those of Slotted_2 cascade. Besides, due to the effect of the blade-end slot jet, the endwall secondary flow flows along the suction surface to the whole-span slot without separation. Then under the blowing effect of the whole-span slot jet, the endwall secondary flow flows to the trailing edge smoothly. As a result, there occurs low loss areas on S4 and S5 planes of Slotted_3 cascade.

By observing the total pressure losses on S6 plane, it can be found that compared with that of the original cascade, the corner separation scopes of the three slotted cascades are effectively reduced. Thus, the scope and extent of the wake losses near endwall of the three slotted cascades are reduced. However, near blade midspan, the mixing effect of the slot jet and the main flow enhances the wake losses, and the wake losses of the three slotted cascades are slightly increased compared with those of original cascade. Compared with those of Slotted_2 and Slotted_3 cascades, the wake losses of Slotted_1 cascade are both greater near blade midspan and endwall, due to the mixing effect of the slot jet and the main flow as well as the flow separation before the trailing edge.

Additionally, because of the mixing effect of the blade-end slot jet and the main flow, the wake losses near the endwall of Slotted_3 cascade are slightly larger than those of Slotted_2 cascade. However, the wake losses near the blade midspan of Slotted_3 cascade are smaller, because the blade-end slot jet better inhibits the secondary flow development from endwall to blade midspan, which reduces the mutual interference between the secondary flow and the main flow.

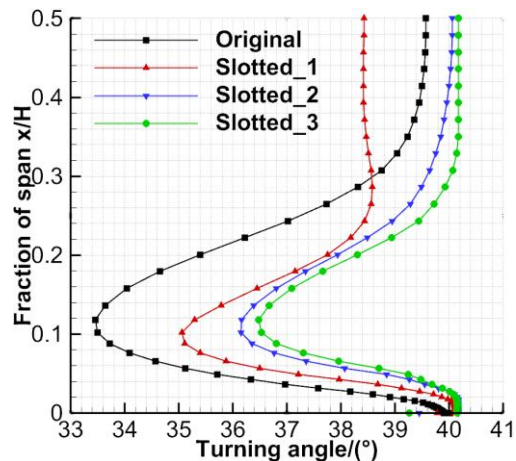


Fig. 7. Spanwise distribution of flow turning angles for original cascade and slotted cascades under 0° incidence angle.

To further analyze the influence of the three slotted schemes on the wake losses, Fig. 9 shows the pitchwise distribution of total pressure recovery coefficients at 50% H and 5% H of S6 plane, which is

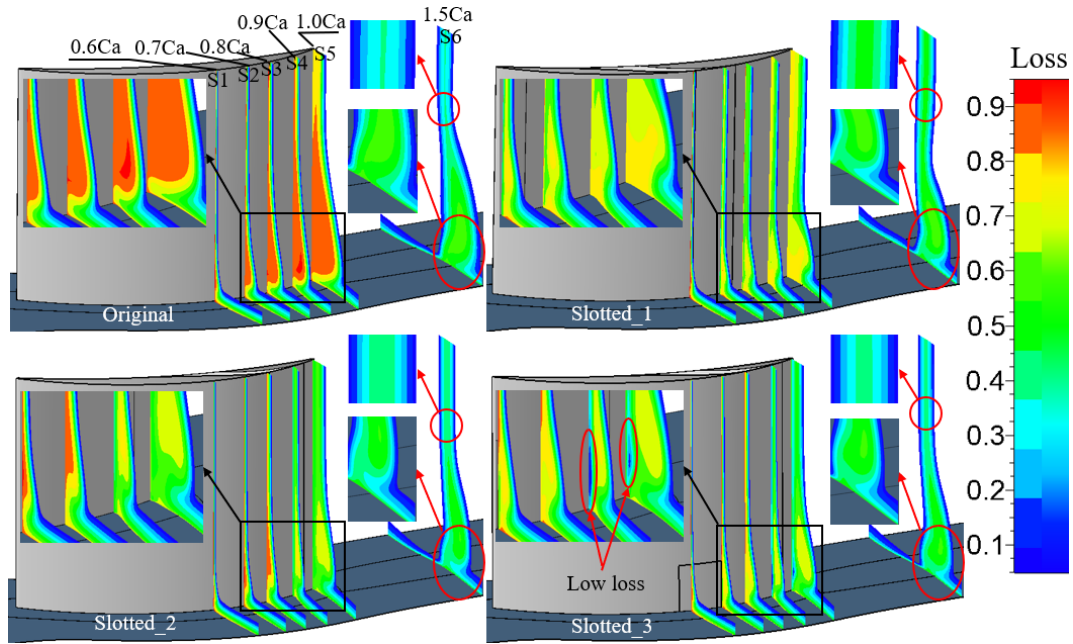


Fig. 8. Passage total pressure loss coefficient contours for original cascade and slotted cascades under 0° incidence angle.

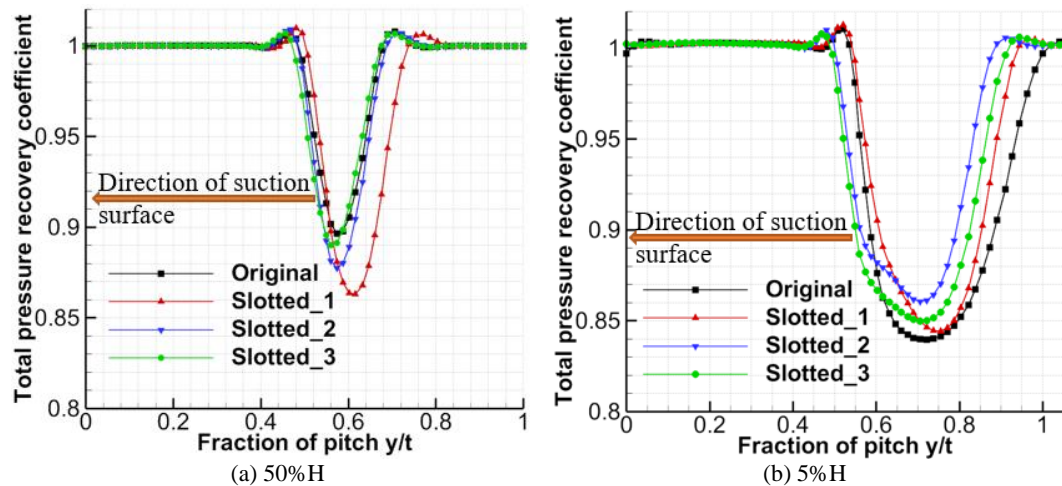


Fig. 9. Pitchwise distribution of total pressure recovery coefficients for original cascade and slotted cascades under 0° incidence angle.

located at 50%*C* downstream of the blade trailing edge. The definition of total pressure recovery coefficient is shown in Eq. (2). As shown in Fig. 9(a), at 50%*H* of *S6* plane, the scopes of low total pressure recovery coefficients corresponding to the three slotted cascades are larger than that of original cascade, and their total pressure recovery coefficients at the lowest point are also lower. That is, the scopes of the wake losses of the three slotted cascades are increased compared with that of original cascade at blade midspan. It can be found that, consistent with the analysis of *S6* plane in Fig. 8, since the separation degree of original cascade near blade midspan is relatively weak, the mixing effect of the slot jet and the main flow enhances the wake losses. Among the three slotted cascades, the wake losses of Slotted_1 cascade are the largest, while those of Slotted_3 cascade are the smallest. As

shown in Fig. 9(b), at 5%*H* of *S6* plane, the wake losses of the three slotted cascades are reduced compared with those of original cascade. But due to the mixing effect of the blade-end slot jet and the main flow, the wake losses of Slotted_3 cascade are slightly greater than those of Slotted_2 cascade.

$$\sigma = \frac{P_{02}}{P_{01}} \quad (2)$$

By observing the central locations of the wake losses in Fig. 9(a) and (b), it can be found that compared with that of original cascade, the center of the wake losses at 50%*H* of Slotted_1 cascade moves toward the pressure surface direction, while that at 5%*H* moves toward the suction surface direction. That is, the deviation angles of Slotted_1 cascade are increased at 50%*H* and decreased at 5%*H*, which is

consistent with the analysis of Fig. 7. In addition, the centers of the wake losses of the other two slotted cascades at 50%H and 5%H move toward the suction surface direction. It means that compared with those of original cascade, the deviation angles of Slotted_2 and Slotted_3 cascades are reduced, and the flow turning angles are increased. Both of the Slotted_2 and Slotted_3 schemes can enhance the pressure diffusion capacity of the cascade.

3.2 Performance Analysis at Wide Range of Incidence Angles

Due to the variable working conditions of aeroengine, the compressor blades don't work only under a certain incidence angle, it is necessary to perform performance analysis on the slotted cascades at wide range of incidence angles. Figure 10 shows the incidence angle characteristics of the four cascades in incidence angle range of -8° to 6.5° . It can be found that the losses of Slotted_1 cascade are smaller than those of original cascade only under positive incidence angles. As incidence angle increases, the separation degree increases, Slotted_1 scheme has an enhanced suppressing effect on the flow separation. However, in the range of negative incidence angles, the losses of Slotted_1 cascade are larger than those of original cascade. According to above analyses, Slotted_1 scheme has a poor adaptability to wide range of incidence angles.

The losses of Slotted_2 and Slotted_3 cascades are reduced in the full range of incidence angles compared with those of original cascade. Taking Slotted_3 cascade as an example, its operating range of incidence angles is broadened, and its total pressure loss coefficient is decreased by 19.5% under 4° incidence angle, which has the largest reduction. In the full incidence angle range, the losses of Slotted_2 cascade are reduced to the same level as those of Slotted_3 cascade, where Slotted_2 cascade has smaller losses under negative incidence angles, while has larger losses under positive incidence angles. In order to further analyze the superiority of the two slotted schemes, the performance of the two slotted cascades and original cascade will be compared and analyzed below under relatively large positive and negative incidence angles.

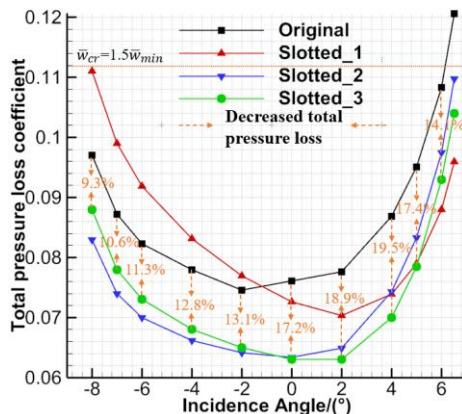


Fig. 10. Total pressure loss coefficients in the full range of incidence angles for original cascade and slotted cascades.

Figure 11 shows the limiting streamlines on the suction surface and endwall of original, Slotted_2 and Slotted_3 cascades under -4° and 4° incidence angles. It can be seen that as incidence angle increases, the degree of the flow separation on the suction surface of original cascade increases, and the starting point of the corner separation line moves toward the leading edge of the blade, the corner separation line also extends to blade midspan and the area of the secondary flow influencing zone becomes larger. In addition, with the increase of incidence angle, the area of the backflow zone near endwall on the suction surface of Slotted_2 cascade increases, and the suppressing effect of the slot jet on the corner separation becomes weaker. Under the two incidence angles, Slotted_3 scheme has a better suppressing effect on the corner separation than Slotted_2 scheme, effectively restraining the development of the secondary flow on the suction surface. However, under the incidence angle of 4° , the reverse pressure gradient is large, thus a small area of backflow zone also appears before the whole-span slot on the suction surface of slotted_3 cascade.

Figure 12 shows the spanwise distribution of pitchwise averaged flow turning angles of the three cascades under -4° and 4° incidence angles. Under the two incidence angles, the flow turning angles of Slotted_3 cascade are almost larger than those of Slotted_2 cascade within the whole span, while there is only 10%H zone under -4° incidence angle, where the flow turning angles of Slotted_3 cascade are slightly smaller. This is caused by the weak separation on the suction surface within 10%-20%H of Slotted_3 cascade (as shown in Fig. 11(a)). Besides, with the increase of incidence angle, the flow turning angles of Slotted_3 cascade are increased more compared with those of Slotted_2 cascade. The reasons are as follows: Since the degree of the corner separation increases as incidence angle increases, compared with Slotted_3 cascade, the suppressing effect of Slotted_2 cascade on the corner separation becomes weaker. For Slotted_2 cascade, the secondary flow develops from endwall to blade midspan on the suction surface before reaching the slot outlet, and the interference between the secondary flow and the main flow intensifies the flow separation, which results in larger deviation angles near blade midspan and endwall.

Figure 13 shows the total pressure loss contours on the plane located at 50%C downstream of the blade trailing edge of the three cascades under -4° and 4° incidence angles. It can be found that as incidence angle increases, the scope of wake losses of original cascade increases. Under the two incidence angles, the wake losses near the endwall of Slotted_2 and Slotted_3 cascades are reduced compared with those of original cascade. Under -4° incidence angle, the corner separation degree of original cascade is relatively weak, due to the mixing effect of the blade-end slot jet and the main flow, the wake losses near the endwall of Slotted_3 cascade are larger than those of Slotted_2 cascade. Near blade midspan, compared with Slotted_2 scheme, Slotted_3 scheme has a better suppressing effect on the development of the endwall secondary flow on the suction surface, which reduces the losses caused by the interference

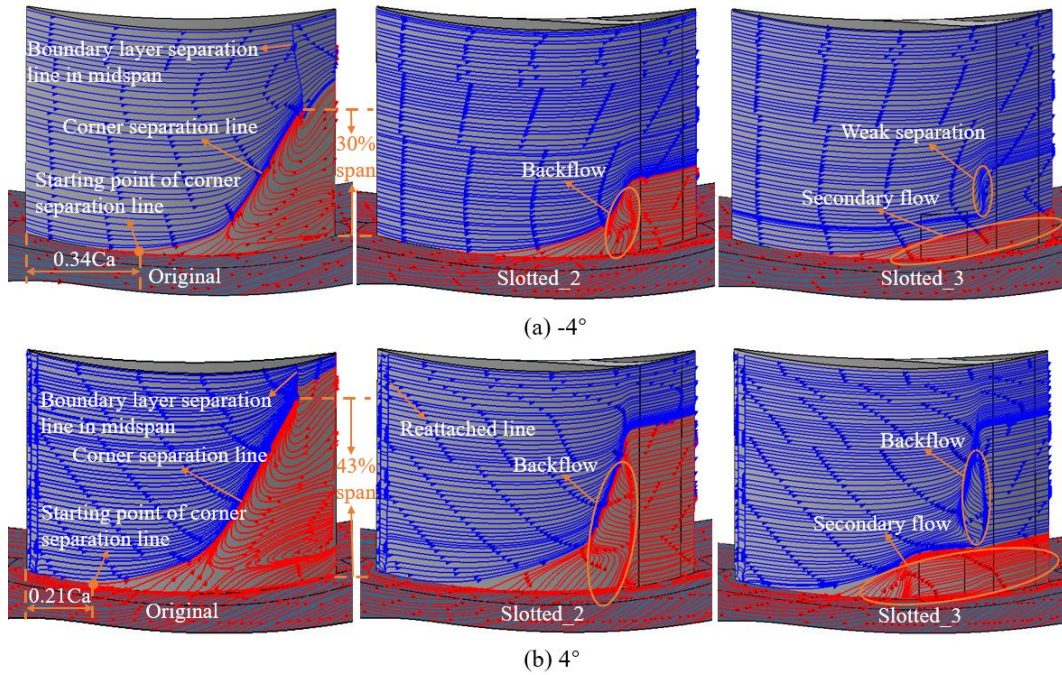


Fig. 11. Limiting streamlines on suction surface and endwall for original, Slotted_2 and Slotted_3 cascades under -4° and 4° incidence angles.

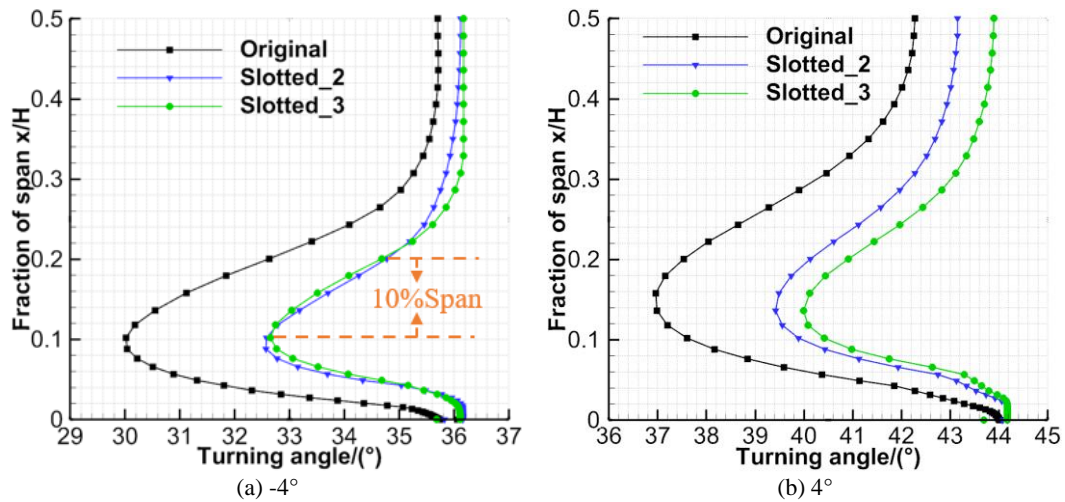


Fig. 12. Spanwise distribution of flow turning angles for original, Slotted_2 and Slotted_3 cascades under -4° and 4° incidence angles.

between the secondary flow and the main flow. Therefore, its wake losses are smaller. However, the same as the situation of 0° incidence angle, the wake losses near the blade midspan of Slotted_3 cascade are still larger than those of original cascade.

Under 4° incidence angle, the corner separation degree of original cascade is serious, Slotted_3 scheme has a significantly better suppressing effect on the corner separation than Slotted_2 scheme. Therefore, the wake losses near the endwall of Slotted_3 cascade are smaller. Additionally, near blade midspan, the wake losses of Slotted_3 cascade are smaller than those of Slotted_2 cascade and slightly larger than those of original cascade. It can be found that with the increase of incidence angle,

Slotted_3 scheme has an enhanced comprehensive suppressing effect on the corner separation and the boundary layer separation on the suction surface of blade midspan.

By observing the central locations of the wake losses of original cascade and the two slotted cascades, it can be found that as incidence angle increases, the center of the wake losses of original cascade moves toward the pressure surface direction, that is, the deviation angles become larger. Under the two incidence angles, the centers of the wake losses of the two slotted cascades move toward the suction surface direction, which means that their deviation angles are decreased, and the flow turning angles are increased. Moreover, the center of the wake losses of

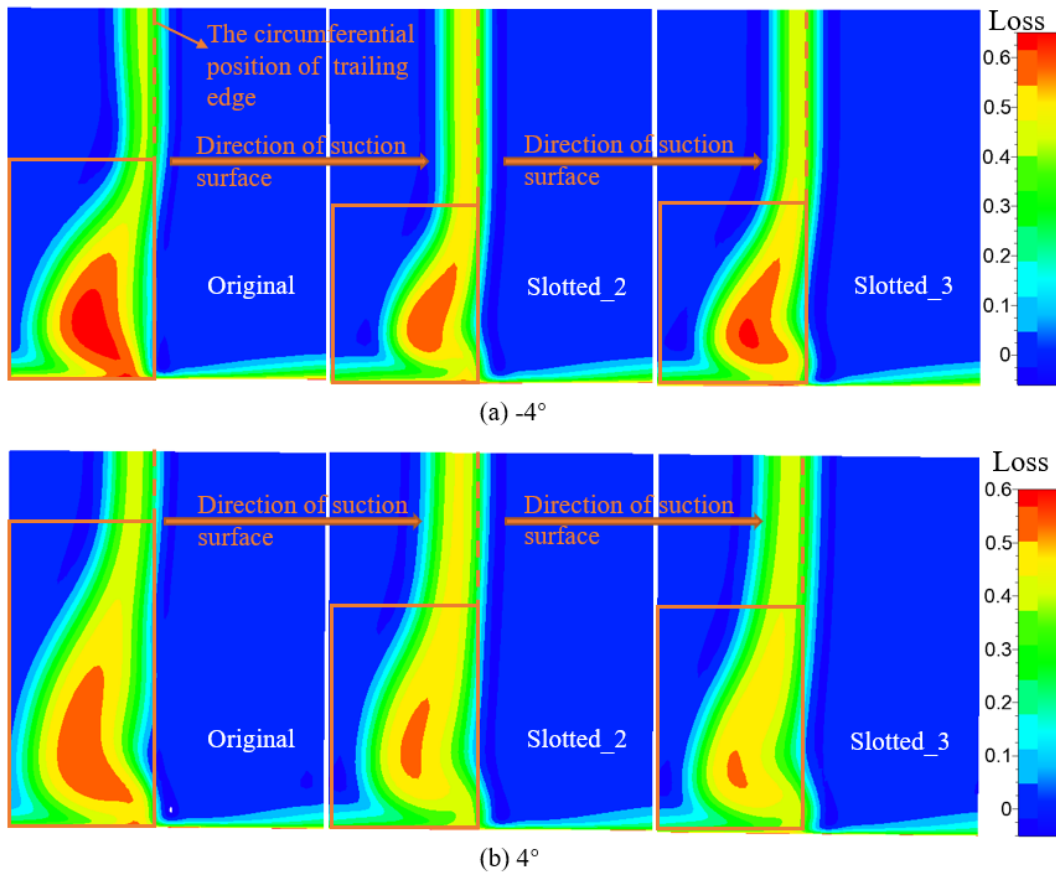


Fig. 13. Total pressure loss coefficient contours for original, Slotted_2 and Slotted_3 cascades under -4° and 4° incidence angles.

Slotted_3 cascade moves further toward the suction surface direction compared with that of Slotted_2 cascade, that is, the flow turning angles of Slotted_3 cascade are larger, which is consistent with the analysis of Fig. 12.

To sum up, due to the mixing losses of the blade-end slot jet and the main flow, the total pressure losses of Slotted_3 cascade are larger than those of Slotted_2 cascade in the range of negative incidence angles. However, in the operating range of incidence angles, the development of the endwall secondary flow on the suction surface of Slotted_3 cascade is effectively suppressed, and the flow turning angles of Slotted_3 cascade are also larger than those of Slotted_2 cascade. Therefore, compared with the whole-span slotted schemes, Slotted_3 scheme has a better comprehensive suppressing effect on the corner separation and the boundary layer separation on the suction surface of blade midspan, which can greatly enhance the pressure diffusion capacity of the cascade.

4. CONCLUSION

A diffusion stator cascade with large camber angle is selected as the research object in this study, and the application of the whole-span slot and the blade-end slots on the cascade has been investigated

numerically, the following main conclusions are obtained:

- (1) The Slotted_1 whole-span slotted scheme has a greatly suppressing effect on the development of the endwall secondary flow on the suction surface, but its slot outlet is located relatively close to the starting point of the corner separation line and is far from the trailing edge, resulting in the flow passing through the slot outlet separates in front of the trailing edge under the reverse pressure gradient. Slotted_1 scheme has a better suppressing effect on the flow separation under positive incidence angles, but in the range of negative incidence angles, the losses of Slotted_1 cascade are larger than those of original cascade. Therefore, Slotted_1 scheme is not adaptable to wide range of incidence angles.
- (2) In the full range of incidence angles, compared with those of original cascade, the total pressure losses of the Slotted_2 whole-span slotted cascade are reduced, and its flow turning angles are increased. However, since the slot outlet is close to the trailing edge, the secondary flow develops from endwall to blade midspan on the suction surface before reaching the slot outlet. The secondary flow

interferes with the main flow and intensifies the flow separation on the suction surface. Slotted_2 scheme has a limited suppressing effect on the corner separation, it is not adaptable to the condition of large positive incidence angles.

- (3) In the full range of incidence angles, the slotted_3 scheme with whole-span slot and blade-end slots can effectively inhibit the development of the endwall secondary flow on the suction surface and basically eliminate the corner separation and the boundary layer separation near blade midspan. The flow turning angles of Slotted_3 cascade are further increased compared with those of Slotted_2 cascade. Moreover, the losses of Slotted_3 cascade are reduced in the full range of incidence angles, its total pressure loss coefficient is reduced by up to 19.5% under 4° incidence angle, thus, the operating incidence angle range of Slotted_3 cascade is broadened. Compared with the whole-span slotted schemes, Slotted_3 scheme has a better adaptability to wide range of incidence angles.

ACKNOWLEDGMENTS

This paper is supported by National Natural Foundation of China (Project No: 51676162, 51790512) and National Science and Technology Major Project (Project No: 2017-II-0001-0013), these supports are gratefully acknowledged.

REFERENCES

- Akcayoz, E., H. D. Vo and A. Mahallati (2016). Controlling Corner Stall Separation with Plasma Actuators in a Compressor Cascade. *Journal of Turbomachinery* 138(8), 081008.
- Beselt, C., M. Eck and D. Peitsch (2014). Three-Dimensional Flow Field in a Highly Loaded Compressor Cascade. *ASME 2014-GT-25947*.
- Cevik, M., H. D. Vo and H. Yu (2016). Casing Treatment for Desensitization of Compressor Performance and Stability to Tip Clearance. *Journal of Turbomachinery* 138(12), 121008.
- Denton, J. D. (1993). Loss Mechanisms in Turbomachines. *Journal of Turbomachinery* 115(4), 621–656.
- Eshraghi, H., M. Boroomand and A. M. Tousi (2016). A Developed Methodology in Design of Highly Loaded Tandem Axial Flow Compressor Stage. *Journal of Applied Fluid Mechanics* 9(1), 83-94.
- Hergt, A., R. Meyer and K. Engel (2012). Effects of Vortex Generator Application on the Performance of a Compressor Cascade. *Journal of Turbomachinery* 135(2), 021026.
- Jones, G. S., A. E. Viken, L. N. Washburn, L. N. Jenkins and C. M. Cagle (2002). An Active Flow Circulation Controlled Flap Concept for General Aviation Aircraft Applications. *AIAA Paper 2002-3157*.
- Kan, X., W. Wu and J. Zhong (2020). Effects of Vortex Dynamics Mechanism of Blade-End Treatment on the Flow Losses in a Compressor Cascade at Critical Condition. *Aerospace Science and Technology* 102(7), 105857.
- Kan, X., W. Wu, L. Yang and J. Zhong (2019). Effects of End-Bend and Curved Blades on the Flow Field and Loss of a Compressor Linear Cascade in the Design Condition. *Journal of Thermal Science* 28(4), 801-810.
- Lei, V. M., Z. S. Spakovszky and E. M. Greitzer (2008). A Criterion for Axial Compressor Hub-Corner Stall. *Journal of Turbomachinery*, 130(3), 031006.
- Liu, Y., J. Sun, Y. Tang and L. Lu (2016). Effect of Slot at Blade Root on Compressor Cascade Performance Under Different Aerodynamic Parameters. *Applied Sciences* 6(12), 421.
- Lord, W. K., D. G. MacMartin and T. G. Tillman (2000). Flow control Opportunities in Gas Turbine Engines. *AIAA 2000-2234*.
- Ma, S., W. Chu, H. Zhang and C. Liu (2018). Impact of a Combination of Micro-Vortex Generator and Boundary Layer Suction on Performance in a High-Load Compressor Cascade. *ASME Turbo Expo: Turbomachinery Technical Conference and Exposition 2A*, V02AT39A011.
- Mao, X., B. Liu and T. Tang (2018). Control of Tip Leakage Flow in Axial Flow Compressor Cascade by Suction on the Blade Tip. *Journal of Applied Fluid Mechanics* 11(1), 137-149.
- Ramzi, M. and G. AbdErrahmane (2013). Passive Control via Slotted Blading in a Compressor Cascade at Stall Condition. *Journal of Applied Fluid Mechanics* 6(4), 571–580.
- Rockenbach, R. W. (1968). Single Stage Experimental Evaluation of Slotted Rotor and Stator Blading, Part IX—Final Report. *NASA-CR-54553*.
- Rockenbach, R. W., J. A. Brent and B. A. Jones (1970). Single Stage Experimental Evaluation of Compressor Blading with Slots and Vortex Generators, Part I—Analysis and Design of Stages 4 and 5. *NASA CR-72626*.
- Tang, Y., Y. Liu and L. Lu (2019). Passive Separation Control with Blade-End Slots in a Highly Loaded Compressor Cascade. *AIAA JOURNAL* 58(1), 85-97.
- Zhang, B., B. Liu, P. Liu and X. Mao (2020). Impact of Boundary Layer Suction on Clearance Leakage Flow in a Cantilever Stator of Transonic Compressor. *Journal of Applied Fluid Mechanics* 13(2), 443-455.
- Zhang, Y., A. Mahallati and M. Benner (2014). Experimental and Numerical Investigation of

Corner Stall in a Highly-Loaded Compressor Cascade. *ASME 2014-GT-27204*.

Zhou, M., J. Zhu and X. Lu (2010). Study of Flow Control Using a Slotted Blade for a Compressor Airfoil at Low Reynolds Number. *ASME 2010-GT-22660*.

Zhou, M., R. Wang, C. Cao and X. Zhang (2008).

Effect of Slot Position and Slot Structure on Performance of Cascade. *Acta Aerodynamica Sinica* 26(3), 400-404.

Zhou, M., R. Wang, Y. Bai and L. Zeng (2009). Numerical Research on Effect of Stator Blade Slot Treatment on Single Stage Compressor Characteristic. *Acta Aerodynamica Sinica* 27(1), 114-118.